

# Supporting Information

## Enhanced Ultrasonically-Assisted Heterogeneous Fenton Degradation of Organic Pollutants over a New Copper Magnetite (Cu-Fe<sub>3</sub>O<sub>4</sub>/Cu/C) Nanohybrid Catalyst

Juan Xiao<sup>∇a</sup>, Junhang Lai<sup>∇a</sup>, Ruchun Li<sup>a</sup>, Xiang Fang<sup>b,c</sup>,  
Dongfang Zhang<sup>b,c</sup>, Panagiotis Tsiakaras<sup>d,e,f,\*</sup>, Yi Wang<sup>a\*</sup>

<sup>a</sup>The Key Lab of Low-carbon Chemistry & Energy Conservation of Guangdong Province, School of Chemical Engineering and Technology, School of Materials Science and Engineering, Sun Yat-sen University, Guangzhou 510275, China.

<sup>b</sup>CCCC Fourth Harbor Engineering Institute Co., Ltd., Guangzhou, 510230, China

<sup>c</sup>Key Laboratory of Durability Technology for Harbor and Marine Structure Ministry of Communication, Guangzhou, 510230, China

<sup>d</sup>Laboratory of Materials and Devices for Clean Energy, Ural Federal University, 19 Mira Str., Yekaterinburg, 620002, Russia.

<sup>e</sup>Laboratory of Electrochemical Devices based on Solid Oxide Proton Electrolytes, Institute of High Temperature Electrochemistry (RAS), Yekaterinburg, 620990, Russia.

<sup>f</sup>Laboratory of Alternative Energy Conversion Systems, Department of Mechanical Engineering, School of Engineering, University of Thessaly, Pedion Areos, 38834, Greece.

---

\*Corresponding authors: Y. Wang ([wangyi76@mail.sysu.edu.cn](mailto:wangyi76@mail.sysu.edu.cn)); P. Tsiakaras ([tsiak@mie.uth.gr](mailto:tsiak@mie.uth.gr))

<sup>1</sup> Equally contributed to the present work.

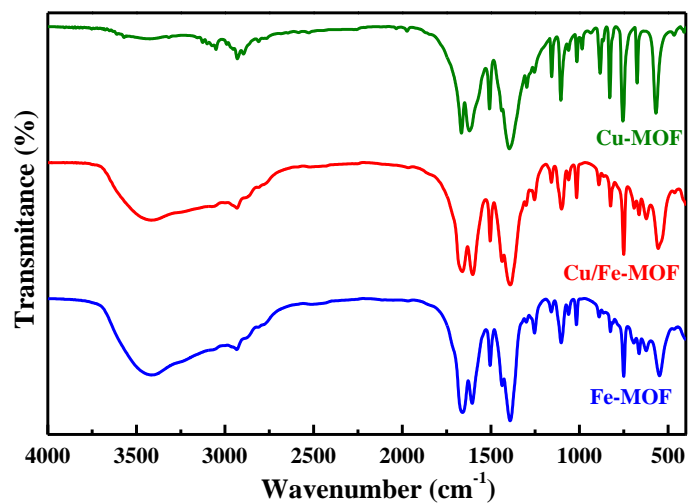


**Figure S1.** FTIR spectra of the as-synthesized MOFs.

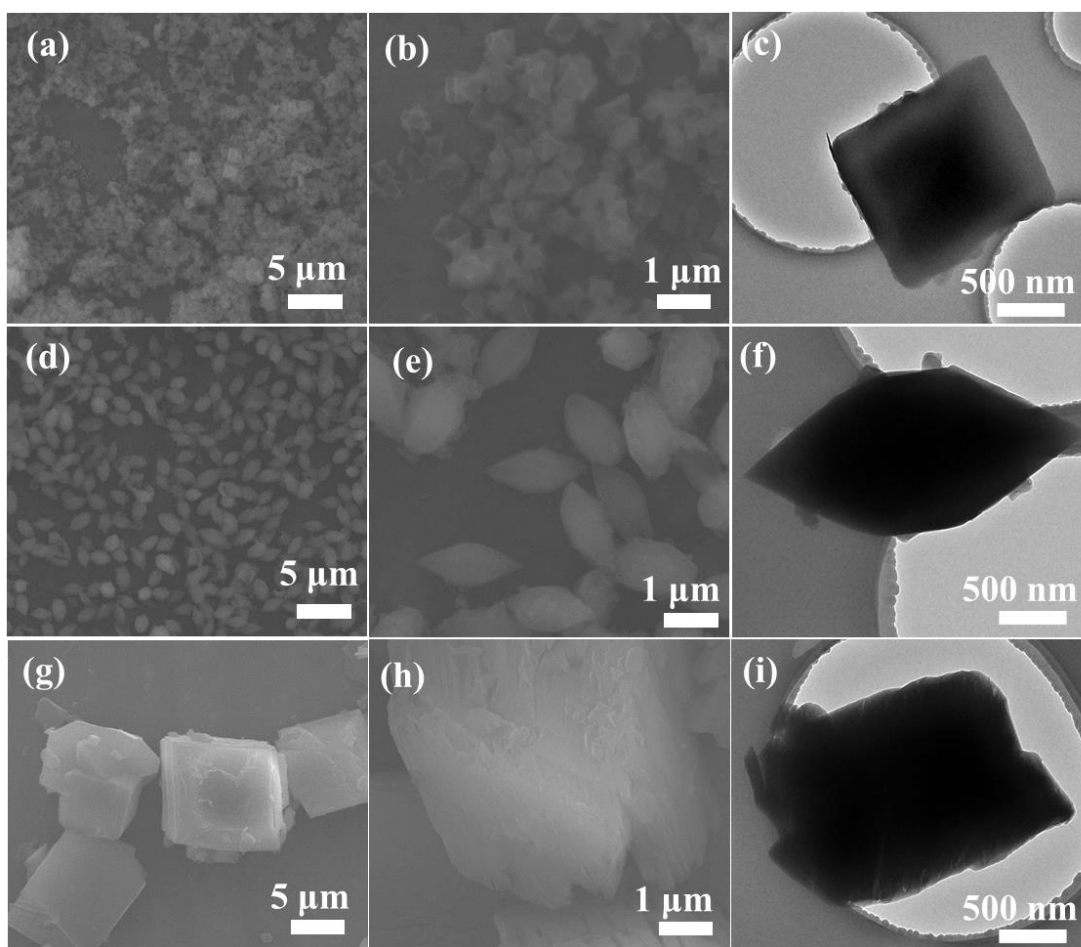


**Figure S2.** (a, b, d, e, g, h) Different magnification SEM and (c, f, i) TEM images of (a,b,c) Fe-MOF, (d, e, f) Cu/Fe-MOF and (g,h, i) Cu-MOF.

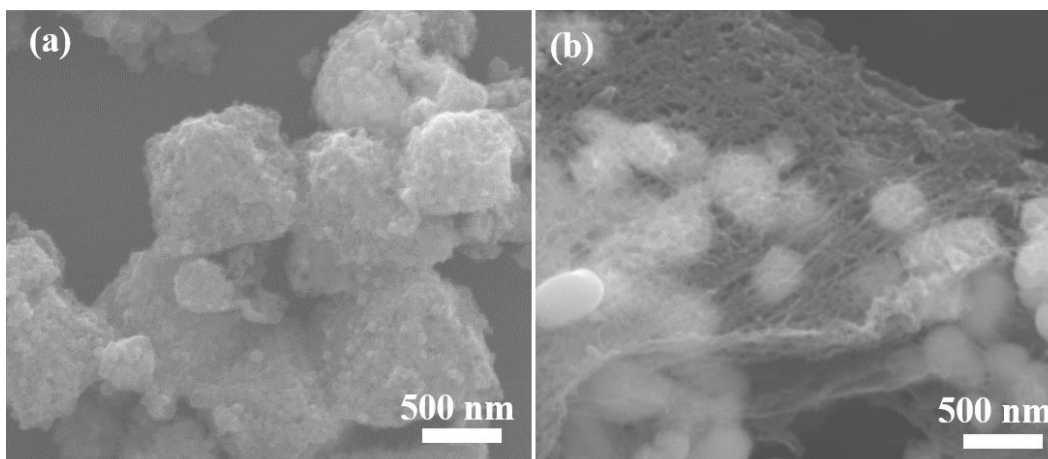


**Figure S3.** SEM images of (a)  $\text{Fe}_3\text{O}_4/\text{C}$  and (b)  $\text{Cu}/\text{C}$ .

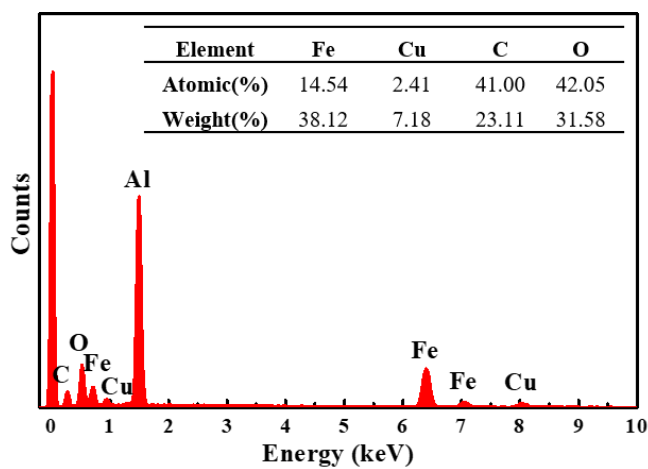


**Figure S4.** EDX spectra of  $\text{Cu-Fe}_3\text{O}_4/\text{Cu}/\text{C}$  along with the corresponding Element content in inset view.

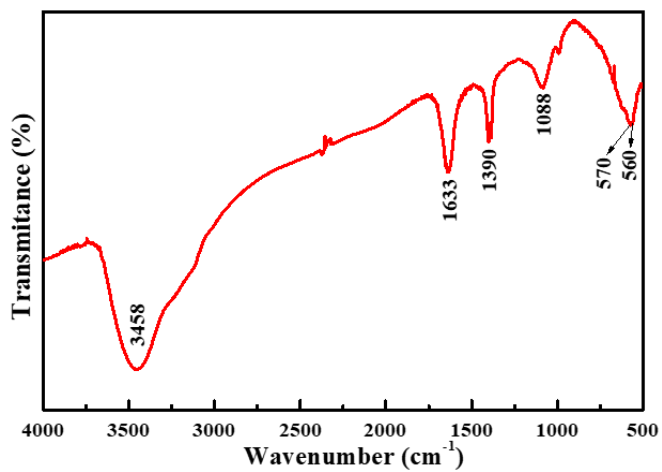


**Figure S5.** FTIR spectrum of the as-prepared  $\text{Cu-Fe}_3\text{O}_4/\text{Cu}/\text{C}$ .

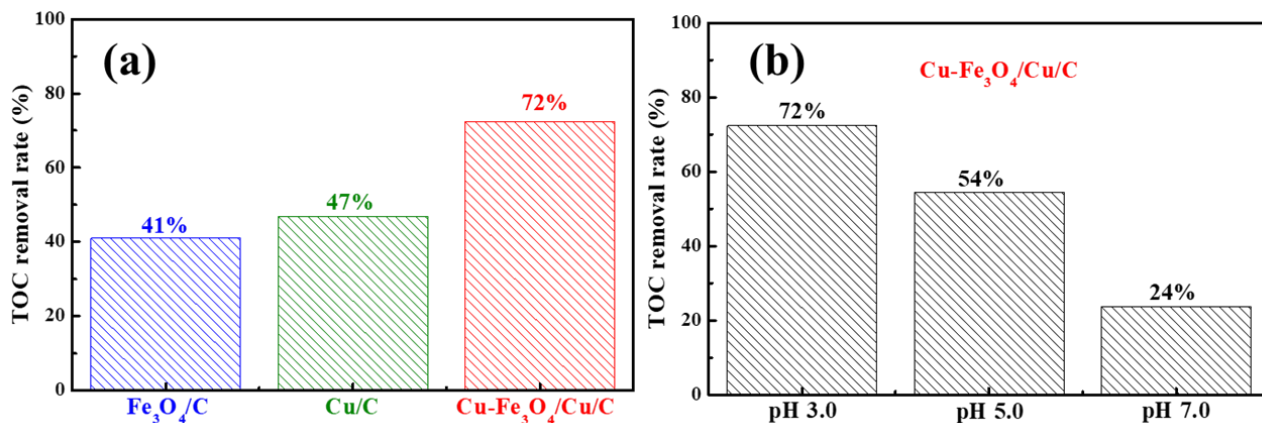


**Figure S6.** TOC removal rate in different (a) catalyst (b) pH systems and for US/H-Fenton degradation of RhB at 3 h of reaction time. Experimental conditions:  $[\text{Fe}_3\text{O}_4/\text{C}] = [\text{Cu}/\text{C}] = [\text{Cu-Fe}_3\text{O}_4/\text{Cu/C}] = 0.1 \text{ g/L}$ ,  $[\text{H}_2\text{O}_2] = 10.0 \text{ mmol/L}$ ,  $[\text{RhB}] = 10.0 \text{ mg/L}$ , pH 3.0.

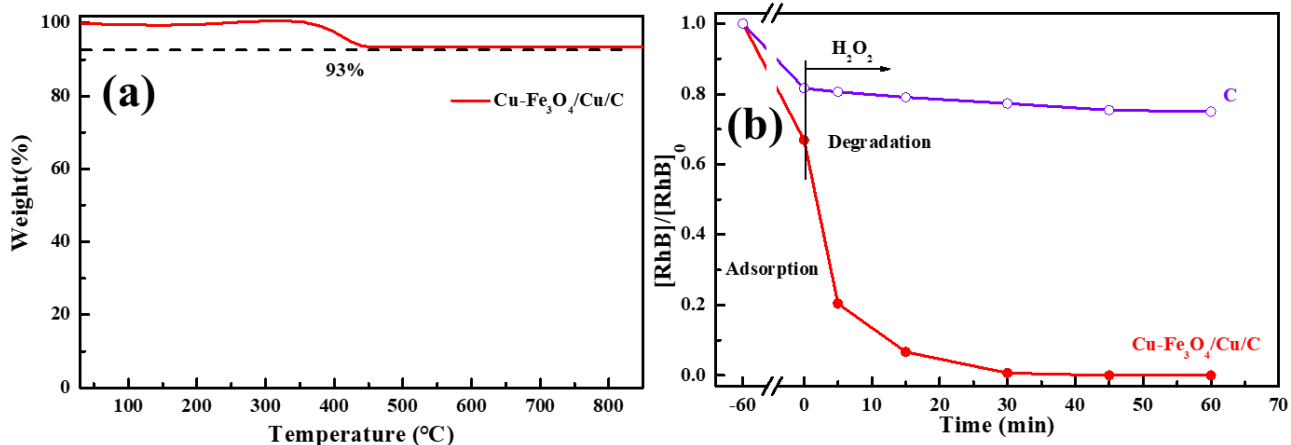


**Figure S7.** (a) TGA curve of Cu-Fe<sub>3</sub>O<sub>4</sub>/Cu/C catalyst in the air atmosphere. (b) RhB degradation efficiency of US/H-Fenton reaction by using C and Cu-Fe<sub>3</sub>O<sub>4</sub>/Cu/C catalysts at pH 3.0. Experimental conditions:  $[\text{C}] = 0.01 \text{ g/L}$ ,  $[\text{Cu-Fe}_3\text{O}_4/\text{Cu/C}] = 0.1 \text{ g/L}$ ,  $[\text{H}_2\text{O}_2] = 10.0 \text{ mmol/L}$ ,  $[\text{RhB}] = 10.0 \text{ mg/L}$ .

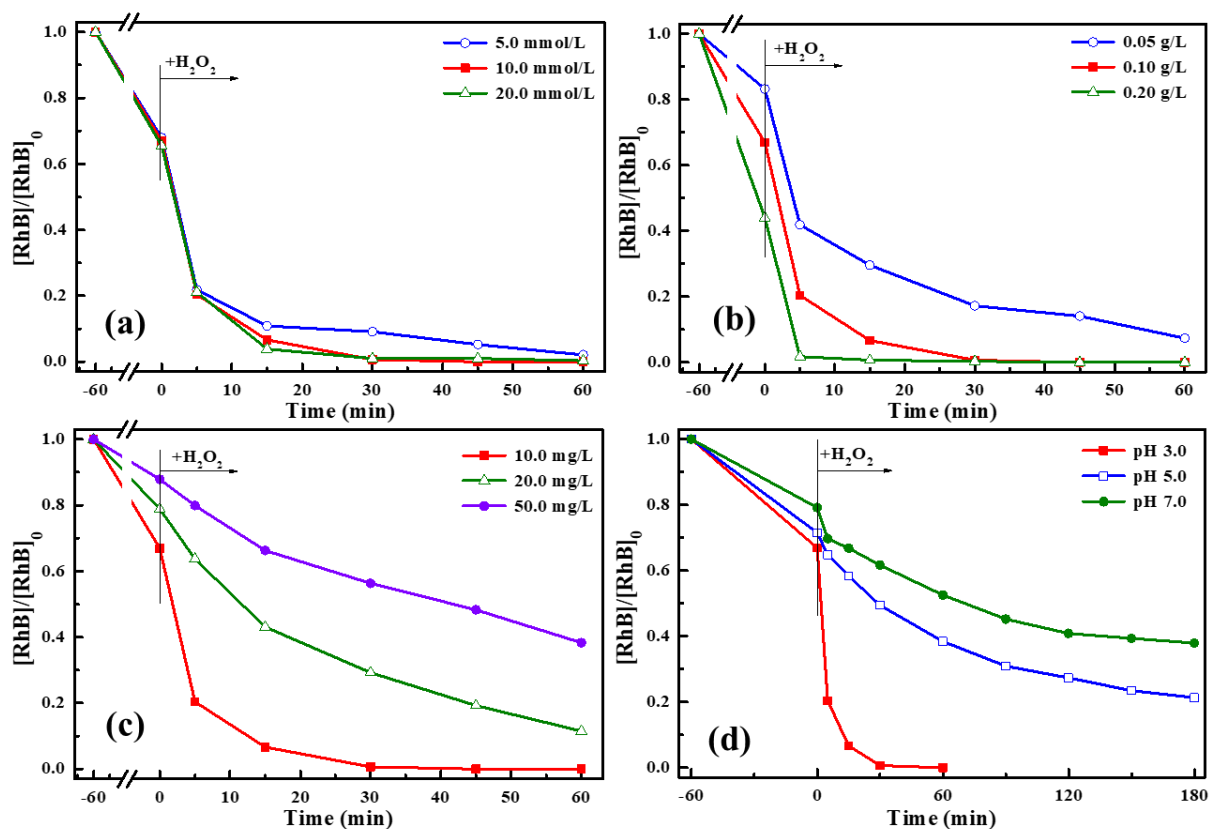


**Figure S8.** Effect of (a)  $\text{H}_2\text{O}_2$  dosage, (b)  $\text{Cu-Fe}_3\text{O}_4/\text{Cu/C}$  dosage, (c) RhB concentration and (d) pH value on RhB degradation during US/H-Fenton process. Other reaction parameters were fixed at  $[\text{Cu-Fe}_3\text{O}_4/\text{Cu/C}] = 0.1 \text{ g/L}$ ,  $[\text{H}_2\text{O}_2] = 10.0 \text{ mmol/L}$ ,  $[\text{RhB}] = 10.0 \text{ mg/L}$ ,  $\text{pH} = 3.0$ .

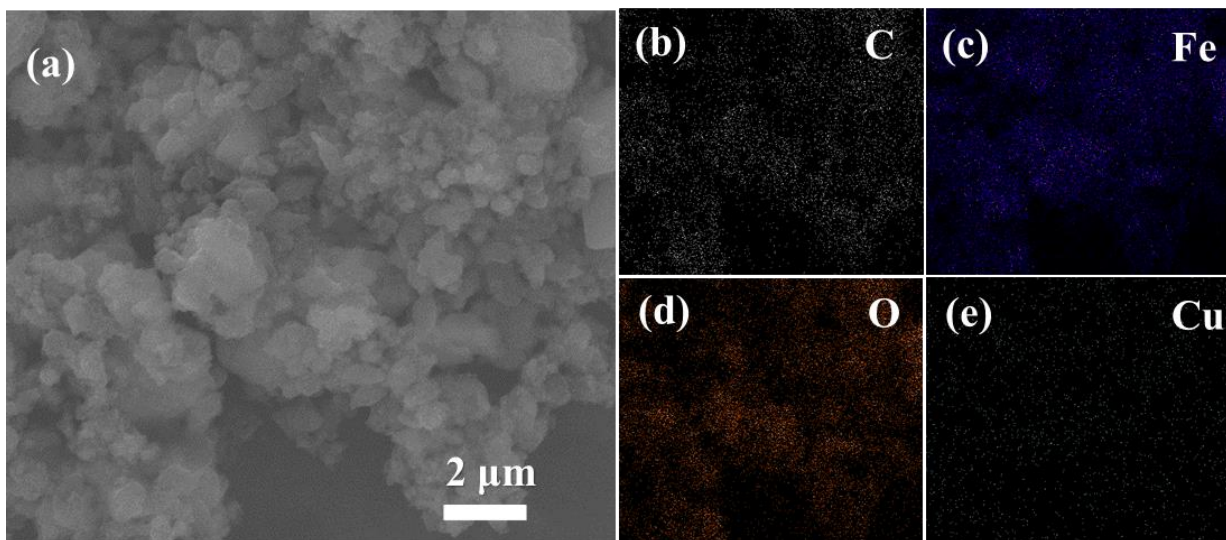


**Figure S9.** (a) SEM image and (b-e) EDS elemental mapping of the used  $\text{Cu-Fe}_3\text{O}_4/\text{Cu/C}$ .

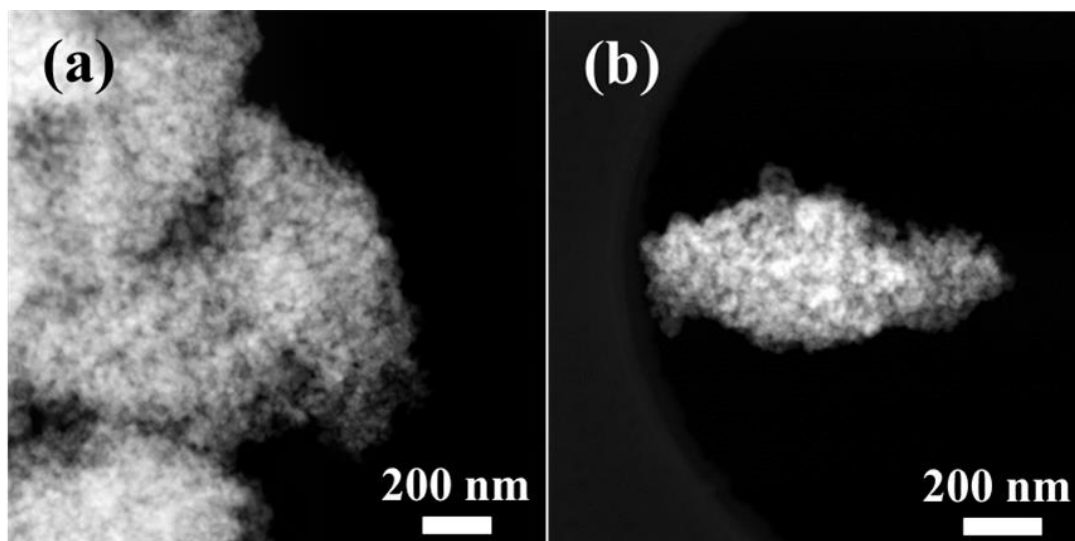


Figure S10. HAADF-STEM images of used Cu-Fe<sub>3</sub>O<sub>4</sub>/Cu/C.

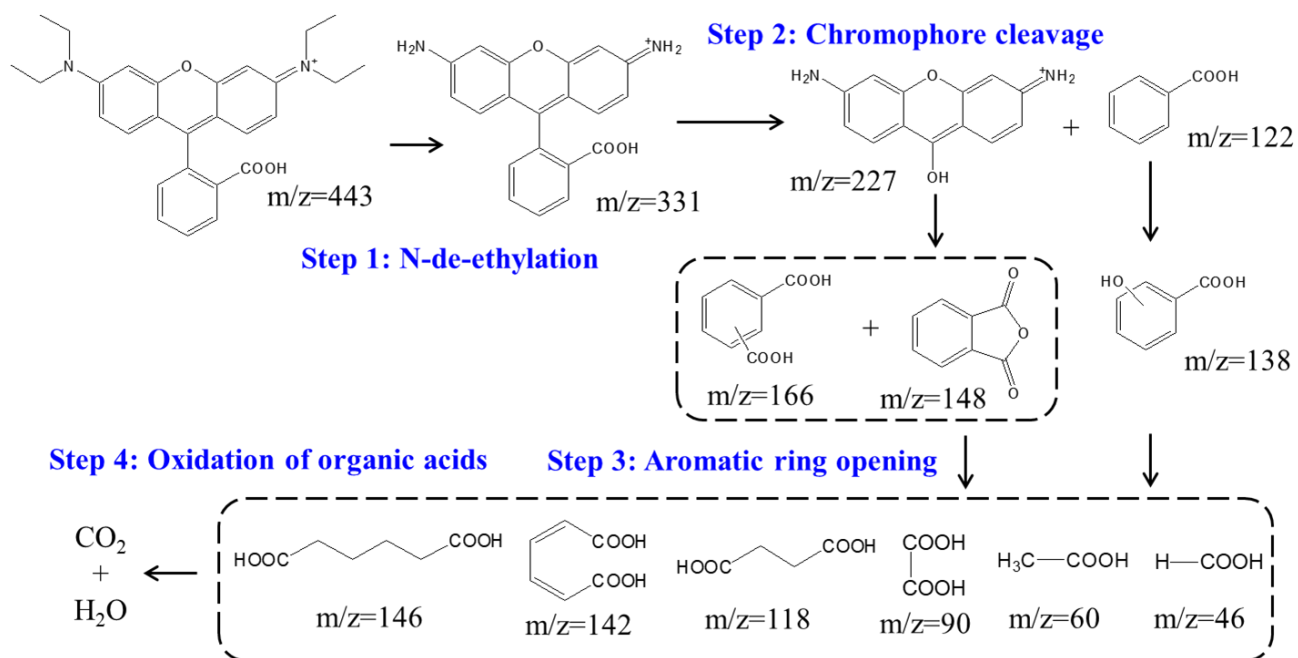


Figure S11. Possible degradation pathway of RhB in US/H-Fenton reaction.

**Table S1.** The comparison on RhB removal rate of Cu-Fe<sub>3</sub>O<sub>4</sub>/Cu/C with other reported heterogeneous catalysts.

Catalysts	Reaction conditions	Removal rate	Reference
$\alpha$ -Fe <sub>2</sub> O <sub>3</sub> /Graphene	pH = 2.9, [cat.] = 0.5 g/L, [H <sub>2</sub> O <sub>2</sub> ] = 6.0 mL/L, [RhB] = 10.0 mg/L, UV irradiation	~90% (60 min)	(1)
Fe <sub>2</sub> O <sub>3</sub>	pH = 2.9, [cat.] = 0.5 g/L, [H <sub>2</sub> O <sub>2</sub> ] = 5.0 mL/L, [RhB] = 10.0 mg/L, UV irradiation	100% (30 min)	(2)
CoFe <sub>2</sub> O <sub>4</sub> @PPy	pH = 7.0, [cat.] = 0.2 g/L, [H <sub>2</sub> O <sub>2</sub> ] = 4.0 mL/L, [RhB] = 10.0 mg/L, UV irradiation	~100% (30 min)	(3)
Cu/C	pH = 3.9, [cat.] = 0.5 g/L, [H <sub>2</sub> O <sub>2</sub> ] = 1.0 mL/L, [RhB] = 10.0 mg/L, US (40 kHz)	~60% (70 min)	(4)
Fe <sub>3</sub> O <sub>4</sub>	pH = 5.0, 55 °C, [cat.] = 0.5 g/L, [H <sub>2</sub> O <sub>2</sub> ] = 3.7 mL/L, [RhB] = 4.8 mg/L	~84% (60 min)	(5)
FeS <sub>2</sub>	pH = 3.0, [cat.] = 1.0 g/L, [H <sub>2</sub> O <sub>2</sub> ] = 0.6 mL/L, [RhB] = 19.2 mg/L	~90% (60 min)	(6)
MgFe <sub>2</sub> O <sub>4</sub>	pH = 3.0, 45 °C, [cat.] = 1.0 g/L, [H <sub>2</sub> O <sub>2</sub> ] = 10.0 mL/L, [RhB] = 10.0 mg/L	~40% (60 min)	(7)
MIL-88A(Fe)	[cat.] = 0.2 g/L, [H <sub>2</sub> O <sub>2</sub> ] = 2.0 mL/L, [RhB] = 10.0 mg/L, UV irradiation	100% (60 min)	(8)
Fe <sub>4</sub> [Fe(CN) <sub>6</sub> ] <sub>3</sub>	pH = 3.5, 35 °C, [cat.] = 0.6 g/L, [H <sub>2</sub> O <sub>2</sub> ] = 1.0 mL/L, [RhB] = 25.0 mg/L, UV irradiation	97% (60 min)	(9)
ZnFe <sub>2</sub> O <sub>4</sub> /C	35 °C, [cat.] = 1.0 g/L, [H <sub>2</sub> O <sub>2</sub> ] = 20.0 mL/L, [RhB] = 5.0 mg/L, UV irradiation	100% (60 min)	(10)
LuFeO <sub>3</sub>	pH = 3.0, 40 °C, [cat.] = 1.0 g/L, [RhB] = 5.0 mg/L, US (40 kHz)	~60% (90 min)	(11)
FePO <sub>4</sub> /N-CNTs	pH = 4.1, [cat.] = 2.0 g/L, [H <sub>2</sub> O <sub>2</sub> ] = 0.9 mL/L, [RhB] = 15.0 mg/L	100% (60 min)	(12)
CuO/Fe <sub>2</sub> O <sub>3</sub> /kaolin	pH = 3.0, [cat.] = 30.0 g/L, voltage = 10.0 V, aeration rate = 0.8L/min, [RhB] = 20.0 mg/L	97% (60 min)	(13)
Cu-Fe <sub>3</sub> O <sub>4</sub> /Cu/C	pH = 3.0, 30 °C, [cat.] = 0.1 g/L, [H <sub>2</sub> O <sub>2</sub> ] = 0.9 mL/L, [RhB] = 10.0 mg/L, US (40 kHz)	~100% (30 min)	This work

## References

- (1) Frindy, S.; Sillanpää, M. Synthesis and Application of Novel  $\alpha$ -Fe<sub>2</sub>O<sub>3</sub>/Graphene for Visible-light Enhanced Photocatalytic Degradation of RhB. *Mater Design*. **2020**, 188, No. 108461.
- (2) Sun, Z. M.; Xiao, C.; Hussain, F.; Zhang, G. Synthesis of Stable and Easily Recycled Ferric Oxides Assisted by Rhodamine B for Efficient Degradation of Organic Pollutants in Heterogeneous Photo-Fenton System. *J. Clean. Prod.* **2018**, 196, 1501–1507.
- (3) Deng, Y. M.; Zhao, X. M.; Luo, J. X.; Wang, Z.; Tang, J. N. Magnetic Recyclable CoFe<sub>2</sub>O<sub>4</sub>@PPy Prepared by in Situ Fenton Oxidization Polymerization with Advanced Photo-Fenton Performance. *RSC Adv*. **2020**, 10, 1858–1869.
- (4) Wang, C. Q.; Wang, H.; Cao, Y. J. Ultrasonic Improvement of Catalytic Decomposition of Rhodamine B in Simulated Wastewater by Functional Waste Printed Circuit Boards via Thermochemical Conversion, *J. Clean. Prod.* **2020**, 253, No. 119921.
- (5) Chen, F. X.; Xie, S. L.; Huang, X. L.; Qiu, X. H. Ionothermal Synthesis of Fe<sub>3</sub>O<sub>4</sub> Magnetic Nanoparticles as Efficient Heterogeneous Fenton-like Catalysts for Degradation of Organic Pollutants with H<sub>2</sub>O<sub>2</sub>. *J. Hazard. Mater.* **2017**, 322, 152–162.
- (6) Diao, Z. H.; Liu, J. J.; Hu, Y. X.; Kong, L. J.; Jiang, D.; Xu, X. R. Comparative Study of Rhodamine B Degradation by the Systems Pyrite/H<sub>2</sub>O<sub>2</sub> and Pyrite/Persulfate: Reactivity, Stability, Products and Mechanism. *Sep. Purif. Technol.* **2017**, 184, 374–383.
- (7) Han, X.; Zhang, H. Y.; Chen, T.; Zhang, M.; Guo, M. Facile Synthesis of Metal-doped Magnesium Ferrite from Sapolite Laterite as an Effective Heterogeneous Fenton-like Catalyst. *J. Mol. Liq.* **2018**, 272, 43–52.
- (8) Fu, H. F.; Song, X. X.; Wu, L.; Zhao, C.; Wang, P.; Wang, C. C. Room-temperature Preparation of MIL-88A as a Heterogeneous Photo-Fenton Catalyst for Degradation of Rhodamine B and Bisphenol a under Visible Light. *Mater. Res. Bull.* **2020**, 125, No. 110806.
- (9) Wang, N.; Ma, W. J.; Du, Y. C.; Ren, Z. Q.; Han, B. H.; Zhang, L. J.; Sun, B. J.; Xu, P.; Han, X. J. Prussian Blue Microcrystals with Morphology Evolution as a High-Performance Photo-Fenton Catalyst for Degradation of Organic Pollutants. *ACS Appl. Mater. Interfaces* **2019**, 11, 1174–1184.
- (10) Wang, F. X.; Chen, Y. L.; Zhu, R. S.; Sun, J. M. Novel Synthesis of Magnetic, Porous C/ZnFe<sub>2</sub>O<sub>4</sub>



Photocatalyst with Enhanced Activity under Visible Light Based on the Fenton-like Reaction. *Dalton Trans.* **2017**, 46, 11306–11317.

- (11) Zhou, M.; Yang, H.; Xian, T.; Li, R. S.; Zhang, H. M.; Wang, X. X. Sonocatalytic Degradation of RhB over LuFeO<sub>3</sub> Particles under Ultrasonic Irradiation. *J. Hazard. Mater.* **2015**, 289, 149–157.
- (12) Wei, L. M.; Zhang, Y.; Chen, S. W.; Zhu, L. P.; Liu, X. Y.; Kong, L. X.; Wang, L. J. Synthesis of Nitrogen-doped Carbon Nanotubes-FePO<sub>4</sub> Composite from Phosphate Residue and Its Application as Effective Fenton-like Catalyst for Dye Degradation. *J. Environ. Sci.* **2019**, 76, 188–198.
- (13) Zhang, B. G.; Hou, Y. P.; Yu, Z. B.; Liu, Y. X.; Huang, J.; Qian, L.; Xiong, J. H. Three-dimensional Electro-Fenton Degradation of Rhodamine B with Efficient Fe-Cu/Kaolin Particle Electrodes: Electrodes Optimization, Kinetics, Influencing Factors and Mechanism. *Sep. Purif. Technol.* **2019**, 210, 60–68.